Modeling Air-Silica Surface Catalysis in Hypersonic Environments using ReaxFF Molecular Dynamics

A THESIS
SUBMITTED TO THE FACULTY OF THE GRADUATE SCHOOL
OF THE UNIVERSITY OF MINNESOTA
BY

Paul E. Norman

IN PARTIAL FULFILLMENT OF THE REQUIREMENTS
FOR THE DEGREE OF
Masters of Science

May, 2010

Acknowledgements

This work was funded by AFOSR Grant FA9550-09-1-0157.

Abstract

The goal of this work is to model surface catalysis in partially dissociated Air-SiO_2 systems, which is of interest for accurately predicting heating on hypersonic vehicles. This is accomplished through molecular dynamics simulations using the ReaxFF potential, which is able to accurately model chemical reactions. The performance of the ReaxFF potential for predicting the bulk structures of several different types of SiO_2 is evaluated, and we find that it most accurately reproduces the structure of β-quartz. Potential energy surfaces for several reactions of interest in catalysis show that the potential may need further training to reproduce results from Quantum Chemical Calculations. Based on a literature review of experimental results and the capabilities of the potential, we choose to model oxygen catalysis on β-Quartz. A methodology for measuring recombination coefficients on a silica surface is developed, and tested for gases at 10atm and 100 atm over the temperature range(600-2000K). We find that recombination coefficients are much higher than those measured experimentally, however, the trend in recombination coefficients is exponential with temperature as seen in experiment.

Contents

List of Tables

List of Figures

Chapter 1

Motivation and Goals

Reentry vehicles, such as the Space Shuttle and the Apollo capsule, enter the Earth's atmosphere at hypersonic velocities. Return from low earth orbit occurs at Mach 25(7km/s), while reentry from Lunar return and direct Mars return occur at even higher speeds. Under these conditions, a bow shock forms in front of the body, which leads to temperatures of several thousand of degrees in the layer between the shock and the surface of the vehicle. Such high temperatures lead to the vibrational excitation and dissociation of diatomic molecules. At the low gas densities characteristic of high altitude hypersonic flight, the gas can diffuse through the boundary layer and reach the surface of the vehicle in a partially dissociated, non-equilibrium state. The surface of the vehicle can act as a catalyst for the exothermic recombination of dissociated species, increasing the heat flux to the vehicle's surface. Studies have shown that heterogeneous catalysis can contribute up to 30% of the total heat load[3] for earth reentry, and that the stagnation point heat flux for Mars entry could vary by a factor of three between the assumptions of highly and weakly catalytic wall[4]. To reliably design thermal protection systems(TPS) for reentry vehicles, as well as other hypersonic vehicles like scramjets, it is important to quantify the aerothermal heating that vehicles need to withstand. Despite a large body of experimental work on surface catalysis for silica surfaces[5, 6, 7, 8, 1, 9], there is still uncertainty in precise temperature, pressure, and gas composition dependence of heating due to heterogeneous surface catalysis[10].

The goal of this research is to develop a surface catalysis model for partially dissociated Air interacting with amorphous SiO_2, which is a significant component in

both ablative and reusable heat shields. Specifically, our objective is to determine recombination coefficients of oxygen and nitrogen, and to determine the rates of various reaction mechanisms, including adsorption, desorption, and recombination. If such rates are accurately obtained, they can be incorporated via surface boundary conditions into large scale Computational Fluid Dynamics(CFD) simulations of full vehicles. To find these rates, we will use reactive molecular dynamics(MD) simulations with the ReaxFF potential[11], which naturally allows bond formation/breaking to occur during the course of a molecular dynamics simulation.

This work specifically focuses on the validation of ReaxFF for different types of SiO_2, and a methodology to obtain recombination coefficients from MD simulations.

Chapter 2

Literature Review

Experimental Review

There has been extensive experimental work done investigating Air - SiO_2 catalysis for a variety of forms of SiO_2 over a range of temperatures and pressures[5, 6, 7, 8, 1, 9]. In most cases experiments measure recombination coefficients, which are defined as the the fraction of impinging atoms that recombine at the surface:

$$\gamma_a = \frac{F_{recombining,a}}{F_{incident,a}} \tag{2.1}$$

Another quantity of interest in experiments is the thermal accommodation coefficient, which accounts for the possibility that not all of the energy produced by a surface recombination is transferred to the surface phonons:

$$\beta = \frac{\Delta H_{ph}}{\Delta H_{rec}} \tag{2.2}$$

A value of $\beta < 1$ corresponds to newly formed molecules leaving the the surface in vibrationally and rotationally excited states[12]. Some experiments measure γ from the heat load on the surface[13], assuming that $\beta = 1$. However, there is experimental evidence that not all of the energy produced by recombination is transferred to the surface[1, 14]. Additionally, it is possible for processes other than recombination, such as the quenching of excited oxygen and nitrogen molecules (which are present under experimental conditions[12]), to increase the heat flux to the surface. Thus, measurements of γ from experiments measuring surface heating with the assumption(β=1) will

be regarded with caution. Generally, we will focus on experiments that measure γ from surface loss coefficients, which are calculated by measuring the change in concentration of a recombining species near a catalytic surface. Note that a surface loss coefficient only contains information about the efficiency of a surface of removing atomic species from the gas phase, and that recombination coefficients are derived from these under the assumption that all atoms lost to surface eventually leave the surface in a recombined state.

The eventual goal of our research is to model surface catalysis on amorphous SiO_2. However, because of the availability of oxygen recombination coefficients on quartz, we have chosen to initially study surface catalysis of oxygen on quartz. Table 2.1 shows a variety of experimental results on quartz. The survey of experimental data in the work by Bedra et al.[15] was useful for constructing this table.

Gas/Setup	Press.(Pa)	Temp.(K)	γ	Reference
O_2/Side Arm	27	920-1250	$2.0\text{x}10^{-4}$ - $3.8\text{x}10^{-4}$*	Kim and Boudart[6]
O_2/Side Arm	40	400-900	$2.5\text{x}10^{-4}$	Marschall[8]
O_2/Plasmatron	$1\text{x}10^{4}$	500-900	$3.0\text{x}10^{-3}$**	Kolesnikov[13]
Air/MOSEX	200	850-1435	$5.5\text{x}10^{-3}$ - $1.36\text{x}10^{-2}$	Balat[1]
O_2/Flowtube	530	770,1110	$2.\text{x}10^{-4}$,$5\text{x}10^{-4}$	Berkowitz[16]

*Scaled by a roughness factor of 2.4.

**Scaled by β.

Table 2.1: Recombination Coefficients for Oxygen on Quartz

Throughout the experiments in Table 2.1, it is observed that recombination coefficients increase with temperature. At higher temperatures(T>750K), recombination coefficients tend to obey an Arrhenius relation $\text{Ae}^{-E_a/RT}$. E_a is referred to as the activation energy, although it should be noted that because γ is a composite of all processes happening on the surface, this value may include the the activation energies of many individual mechanisms. The activation energy for oxygen recombination on quartz was found to be .185 $\pm$ .006 eV in the work by Kim and Bourdart[6] and .166 $\pm$ .02 eV in the work by Balat[1]. At lower temperatures, recombination coefficients do not obey an Arrhenius relation but display a more complex behavior[9].

Computational Review

There have also been several computational studies with the goal of modeling surface catalysis on SiO_2. In one series of studies[17, 10, 18, 19], the authors used an empirical force field and later a Density Function Theory(DFT) based potential to study recombination on (001)β-quartz and (001)β-Cristobalite surfaces. To calculate recombination and adsorption/reflection probabilities, the authors used a semi-classical Time-Dependent Collision Dynamics, where the dynamics of gas phase atoms are described classically, and lattice phonons of the surface are quantized. Recombination coefficients were calculated by placing one oxygen atom on the surface and the adding another oxygen atom above the surface with a given velocity and incident angle. Recombination events were counted when an O_2 formed due to a collision and left the surface, and γ was calculated from many such collisions. The authors reported recombination coefficients at 1000K of $\gamma = .008$ on β-quartz and γ=.0123 on β-Cristobalite[10], which are very close to experimentally measured values. However, these recombination coefficients did not follow an exponential trend with temperature[18].

In another series of studies by Arasa et al.[20, 21, 22] the authors created an interpolated potential energy surface for oxygen above the (001) surface of β-Cristobalite with DFT. The potential energy surface was used to calculate adsorption energy of oxygen, as well as a transition state energy barrier for oxygen recombination. Using classical dynamics and a similar method as above to calculate γ, the authors found a recombination coefficient of $\gamma = .01$ at 1000K, which is in good agreement with experiment. Additionally, the recombination coefficients obeyed an Arrhenius type relation with temperature. The activation energy of the exponential fit was .24eV, which compared favorably with the DFT transition state energy of recombination(.28eV), and the activation energy from experimental results (.285eV)[1]. However, it should be noted the experimentally measured activation energy is fit from the change in recombination coefficients with temperature, and that the activation energy of one step in the process might not be enough characterize the trend in recombination coefficients. Also, the authors only considered normal collisions when calculating recombination coefficients and noted that collisions at off-normal incidence resulted in lower values.

In both series of studies, recombinations were defined by an O_2 molecule leaving the surface almost immediately($\sim$2.5ps) after a gas phase oxygen atom collided with

an oxygen atom adsorbed on the surface. Both studies saw a high probabilities(.5 in [22]) of an oxygen molecule forming on the surface, but not immediately desorbing. If molecular oxygen formation of the surface was included, the recombination coefficients in these computational studies would be much higher.

This research expands upon the work of Cozmuta, who studied surface catalysis on SiO_2 using ReaxFF[2] molecular dynamics. Specifically, the author considered the effects of temperature and pressure on the interaction of atomic nitrogen and oxygen with several silica surfaces. Serial molecular dynamics simulations were performed with the ReaxFF potential at pressures of 10atm and 100atm at temperatures ranging from 300-1900K. The simulation domain was initialized with a gas phase populated with atomic oxygen and nitrogen surrounding a thermostatted slab of silica(shown in Fig. 2.1), and the number of atoms in the simulation was kept constant with time. In these simulations, equilibrium was rapidly achieved over the course of 300-600ps. The majority of gas phase atoms adsorbed to the surface, while the rest recombined on the surface and returned to the gas phase. The changing concentration of species with time is shown in Fig. 2.1.The author noted that the main trend to be extracted from the simulations was that oxygen strongly adsorbed to the surface compared to nitrogen, and a significant amount of molecular nitrogen formed in the gas phase. In this work we will simplify the problem by only considering oxygen interactions with the surface. In addition, we will take a slightly different approach in simulating the gas phase region by only considering the flux of an ideal gas to the surface, thereby maintaining a constant composition, temperature, and pressure in the gas phase.

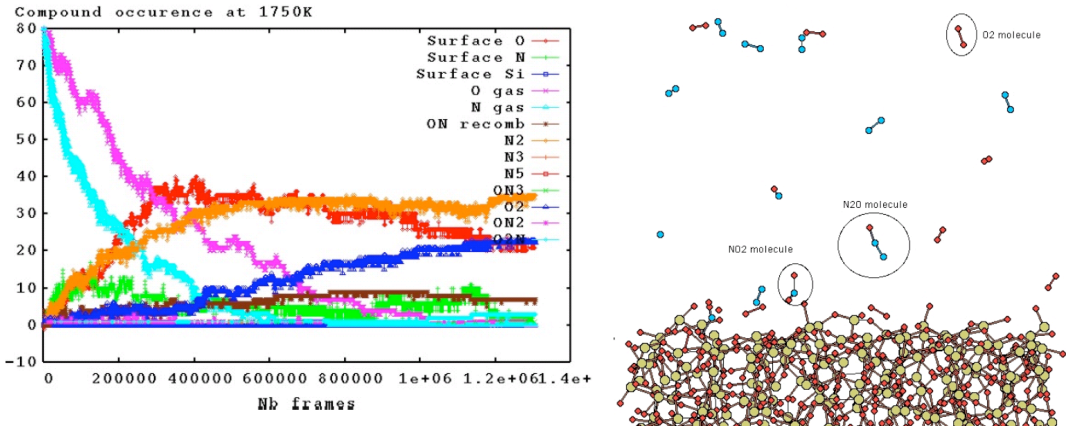

(a) Species concentration with time

(b) Amorphous SiO_2 interacting with N O gas

Figure 2.1: ReaxFF MD Simulations from[2].

Chapter 3

Surface Catalysis Model

Current State of the Art

In modern CFD codes, there are various approaches to account for the heat flux at a wall due to surface catalysis. As a lower bound for the heat flux, a non-catalytic wall boundary condition is used. This condition assumes that the surface does not change the chemical composition of the gas. The upper limit of heating due to surface catalysis is calculated from a super catalytic wall boundary condition, which assumes that species diffusing to the wall recover their free stream enthalpy and mass fractions. However, it is possible that this boundary condition is unphysical. Because the mass fractions of species are imposed at the wall, the net flux of a species may be higher than what is allowed by kinetic theory[4]. To model heating in between these cases, the recombination of gas phase species on the surface is calculated from experimentally based recombination coefficients where γ=const. or γ(T). The heating on the surface is found using the assumption that all of the energy released by recombinations is transferred to the wall($\beta = 1$). However, there are some drawbacks to using recombination coefficients because they only account for the net effect of the surface on the gas, and not the underlying mechanisms contributing to catalysis. For example, in a system with both atomic oxygen and nitrogen, reactions of the form O + N(S) $\rightarrow$ NO + (S) and O + O(S) $\rightarrow$ O_2 + (S) could both deplete atomic oxygen in the gas phase. Thus, the recombination coefficients(γ_O, γ_{NO}) for these two processes are not independent, and an additional preference factor would be need to fully describe the reactions[4]. In addition,

for a complete description of catalysis on the surface, γ should be a function of local temperature, pressure, and gas phase composition. In this work we will instead describe surface catalysis with a set of mechanisms, which allows a fundamental description of surface catalytic processes from a molecular point of view.

Finite Rate Catalytic Boundary Condition

For a description of surface catalysis, we will use a set of mechanisms, similar to those defined by Deutschman et al.[23]. In a non-exhaustive list of mechanisms, shown in Table 3.1, (S) is defined as a vacant chemisorption site, (S_*) is a vacant physisorption site, and A_i is any atomic species in the gas phase. Chemisorption is defined as the formation of a chemical bond between a gas phase atom and a surface site, whereas physisorption involves a much weaker bond forming due to a Van der Waals interactions. While the rates of some of these mechanisms have been tabulated[23], their values are derived from empirical data with large uncertainties.

$A_i + (S) \rightarrow A_iS$	atomic chemisorption
$A_i + (S_*) \rightarrow A_iS_*$	atomic physisorption
$A_{2i} + (S) \rightarrow A_{2i}S$	molecular chemisorption
$A_{2i} + (S_*) \rightarrow A_{2i}S_*$	molecular physisorption
$A_{2i} + (S) + (S) \rightarrow A_iS + A_iS$	dissociative chemisorption
$A_iS \rightarrow A_i + (S)$	atomic chemidesorption
$A_iS_* \rightarrow A_i + (S_*)$	atomic physidesorption
$A_{2i}S \rightarrow A_{2i} + (S)$	molecular chemidesorption
$A_{2i}S_* \rightarrow A_{2i} + (S_*)$	molecular physidesorption
$A_i + A_iS \rightarrow A_2 + \mathrm{S}$	Eley-Rideal(ER) recombination
$A_iS_* + \mathrm{S} \rightarrow S_* + A_i\mathrm{S}$	physisorbed to chemisorbed
$A_iS + A_iS \rightarrow A_2 + \mathrm{S}$	Langmuir Hinshelwood(LH) recombination

Table 3.1: Mechanisms for Surface Catalysis

Of particular interest are the two recombination pathways: Eley-Rideal(ER) recombination and Langmuir Hinshelwood(LH) recombination. In ER recombination, a gas phase atom impacts an adsorbed atom and recombines with it. In LH recombination, surface diffusion enables two atoms adsorbed on the surface to encounter each other

and recombine. Some processes, such as adsorption and Eley-Rideal(ER) recombination, are expected to proceed relatively quickly and are good candidates for molecular dynamics simulations. For slower mechanisms, like desorption and LH recombination, accelerated molecular dynamics and other techniques may be required. Once the rates of the reactions in Table 3.1 have been determined, they can be integrated into a computational fluid dynamics simulation as a boundary condition as shown by Valentini, Schwartzentruber and Cozmuta[24]. Such an approach ultimately relies on the accuracy of the chemical rate data. The goal of this research is to determine the rates of the above mechanisms as a function of temperature and pressure.

Chapter 4

ReaxFF: Description and Validation

Description

ReaxFF$_{SiO}$ is a classical potential parametrized from quantum chemical(QC) calculations which was developed by van Duin and coworkers[11]. There have been many empirical force fields(FFs) developed for various silica structures(see [11] for a list). While these FFs can provide valuable insight into crystal structures and interactions of silica with various organic compounds, they are generally limited to the geometries near the equilibrium structure of the morphology they were designed to reproduce. The ReaxFF$_{SiO}$ force field was developed to provide a consistent description of Silicon and Silicon Oxide bonding over a wide range of crystal structures.

One fundamental difference between ReaxFF and other force fields is that ReaxFF does not used fixed connectivity for chemical bonds. Rather, a bond order term is calculated from the interatomic distances, which are updated at every MD time step. The bond order is a smooth function which goes to zero as the interatomic distance approaches the cutoff radius. Bonding energies(E$_{bond}$), as well as energies associated with bond angles(E$_{val}$) and torsion angles(E$_{tor}$) are all functions of bond order, ensuring that all terms vanish properly when a bond is broken. The complete energy of a system is given by a number of terms, including long range non-bonded terms(such as Coulomb

and Van der Waals interactions):

$$E_{system} = E_{bond} + E_{over} + E_{under} + E_{ip} + E_{val} + E_{pen} + E_{tors} + E_{conj} + E_{vdWalls} + E_{Couloumb} \tag{4.1}$$

Another important aspect of the ReaxFF potential is the geometry dependent charge calculation scheme, which assigns charges to atoms and accounts for polarization effects. For a full description of the ReaxFF force field and its parametrization, we refer the reader to the original work [11]. ReaxFF$_{SiO}$ was validated for a range of silica polymorphs, including α-Cristobalite, Coesite, Stishovite, Trydimite, and α-quartz.

Validation

The eventual goal of this research is to model surface catalysis on amorphous SiO_2. However, because there are both experimental and computational results for simple crystal structures, our initial simulations focus on these. We have investigated the performance of ReaxFF for two polymorphs of SiO_2, α/β-quartz and β-Cristobalite.

β-Cristobalite

β-Cristobalite is a polymorph of SiO_2 that is stable at high temperatures(1750K - 2000K) and atmospheric pressure[25], so it might be a good candidate for modeling recombination on a silica surface under hypersonic conditions. There remains some controversy about its crystal structure; five different structures have been proposed[26, 27, 28, 29, 30, 31]. Recent DFT studies have shown that the fd3m(ideal fcc), and I$\bar{4}$2d(slightly disordered, tetragonal) structures are the two most stable structures[25, 20]. The crystal structure formed from the fd3m unit cell is shown in Fig. 4.1a.

	Experimental[33]	ReaxFF	DFT-GGA[25]	DFT-GGA/PW91[20]
Unit cell (Å)	7.159	7.221	7.268	7.453
Bond Length$_{Si-O}$(Å)	1.55	1.575	1.606	1.614
$\angle$ Si-O-Si (^{o})	180	170.36 ± 1.3	180	180
$\angle$ O-Si-O (^{o})	109.5	109.69 ± 0.85	109.5	109.5
Cohesive Energy(eV/SiO_2)		20.83	23.84	19.66

Table 4.1: Experimental and Computational Results for the crystal structure and cohesive energy of β-Cristobalite.

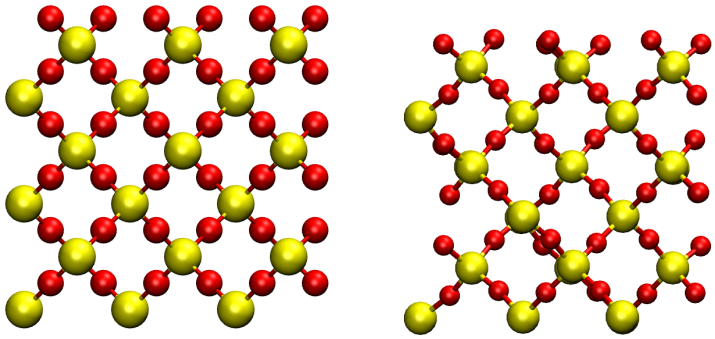

(a) Ideal bulk β-Cristobalite (b) β-Cristobalite after minimization

Figure 4.1: Crystal structure of β-Cristobalite. Silicon atoms are yellow, oxygen atoms are red

Starting with the fd3m unit cell, we performed equation of state(compression/expansion) calculations. This was done by rescaling the unit cell by the desired amount and running a conjugate gradient geometry minimization implemented in LAMMPS[34]. In Fig. 4.2 we can see that ReaxFF predicts a minimum close to the minimum predicted by DFT. However, the change in energy under compression is lower than expected. Additionally, we find that there is some strain energy in the crystal at its minimum configuration: the final two-norm force(which is the length of the global force vector) is $12.7\frac{kcal}{molxAngstrom}$ and the maximum force component is $6.3\frac{kcal}{molxAngstrom}$ for one unit cell. To remove the strain and determine the bulk structure, we performed an isotropic box relaxation minimization on a 6x6x6 crystal created from the unit cell. As shown in Fig. 4.1, the crystal structure produced is slightly disordered with a notable change in the angle of the Si-O-Si bond. The comparison of this crystal structure with DFT and an experiment is given in Table 4.1.

Although ReaxFF does not predict the exact crystal structure of β-Cristobalite, it does predict a somewhat similar structure. The β-Cristobalite crystal structure was not considered in the parametrization of ReaxFF$_{SiO}$. To reproduce the exact crystal structure it may be necessary to slightly retrain/improve the force field. The power of

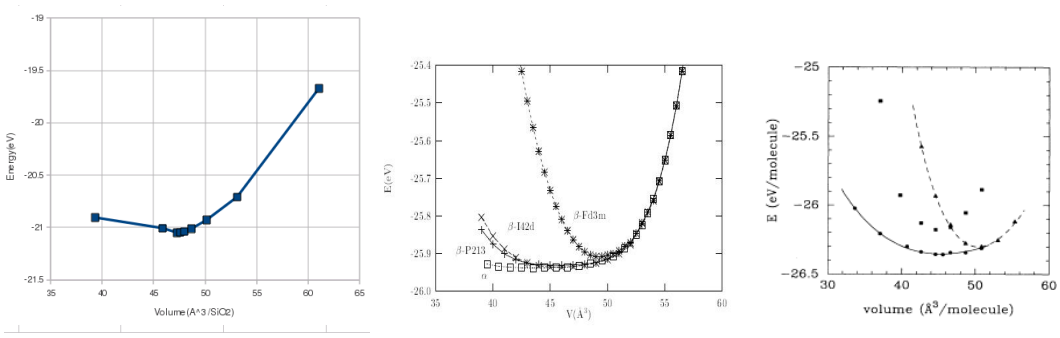

(a) ReaxFF (b) DFT-GGA(stars)[25] (c) DFT-LDA Fd3m (triangles)[32]

Figure 4.2: Equation of State of β-Cristobalite. Plots do not have the same energy zero.

ReaxFF potential is that, if desired, the structure and energy of β-Cristobalite could be added to the training set, thereby improving the performance potential for this problem.

β-Quartz

Quartz is a polymorph of SiO_2 that can occur in two phases: α-quartz and β-quartz. Both are characterized SiO_4 tetrahedra arranged on pairs of helical chains spiraling in the same sense around a hexagonal screw axis. The structure of α-quartz can be considered a distorted form of the the ideal β-quartz, seen as a rigid rotation of the SiO_4 tetrahedra about the (100) axis by $\pm$ 16.2 degrees. There is still some question as to whether the β-phase is no more than a disordered array of small domains of the α phase[25]. The $\alpha \rightarrow \beta$ phase transition occurs at 846K. Equation of state calculations show that ReaxFF predicts degenerate structures for α and β quartz, as seen in Fig. 4.4. In this figure we can also see that ReaxFF does successfully predict the qualitative performance of the two phases under compression and expansion. As shown in Fig. 4.3, the minimized bulk structures of **both** phases closely resemble β-quartz. The crystal structure and cohesive energy were taken from the minimum, and are in reasonable agreement with DFT and experimental measurements as seen in Table 4.2. The largest deviation from experiment is the Si-O-Si angle, which is a 6°(3.8%) difference from experiment. Such agreement with experimental and DFT lends confidence to the ability of ReaxFF$_{SiO}$ to model β-Quartz.

	Experimental[35]	ReaxFF	DFT-GGA[25]	DFT-LDA[25]
a(Å)	4.9977	5.002	5.0845	5.0261
c(Å)	5.4601	5.481	5.5647	5.5124
c/a(Å)	1.0925	1.0957	1.0922	1.0867
V/SiO_2	39.67	38.87	41.53	40.20
Si-O(Å)	1.5895	1.58	1.6142	1.5968
$\angle$ Si-O-Si (^{o})	153.0	159	154.2	154.2
$\angle$ O-Si-O (^{o})	110.1	112.54	109.9	
$\angle$ O-Si-O (^{o})	111.3	112.60	110.4	
$\angle$ O-Si-O (^{o})	107.0	106.70	108.1	
Cohesive Energy(eV/SiO_2)		20.33	23.8242	

Table 4.2: Experimental and Computational Results for the crystal structure and cohesive energy of β-quartz.

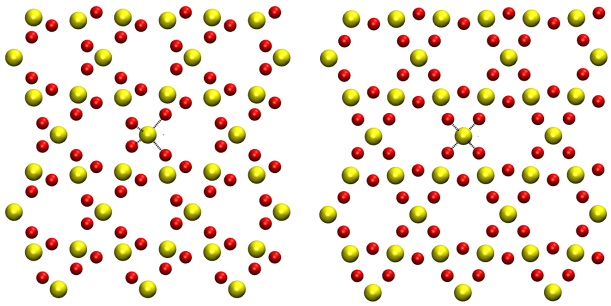

(a) α-quartz top view (b) α-quartz after minimization(β-quartz)

Figure 4.3: The crystal structures of α and β quartz.

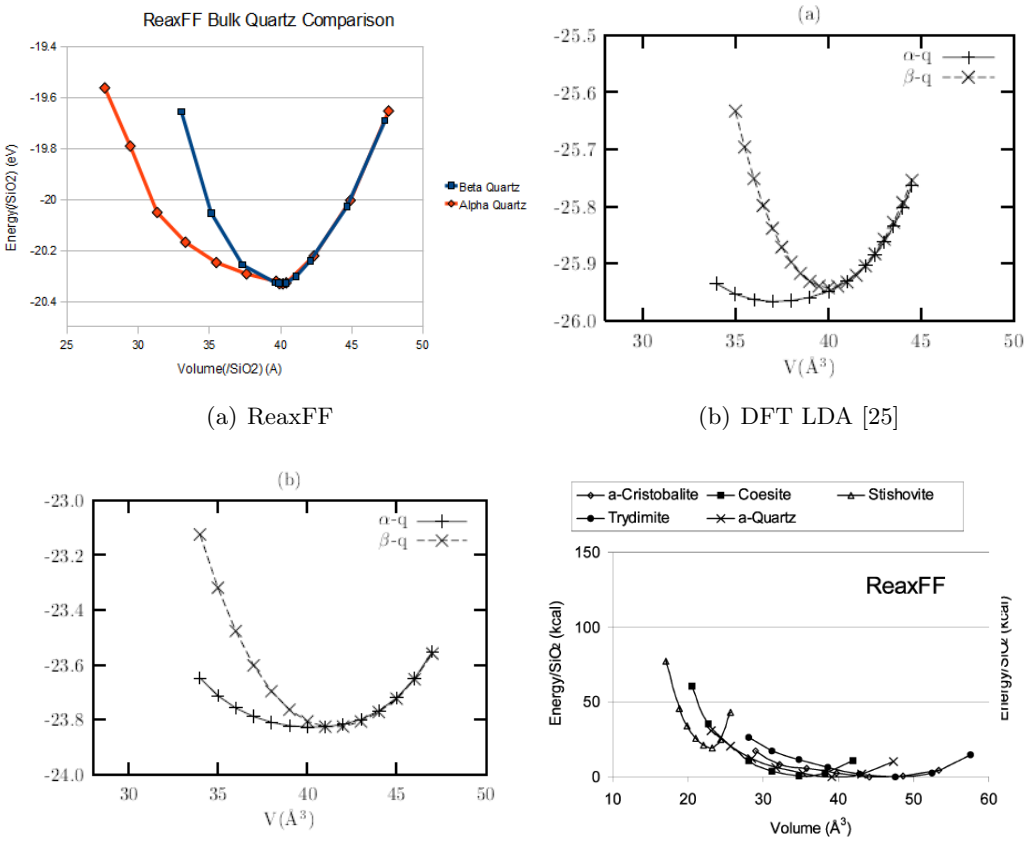

(a) ReaxFF

(b) DFT LDA [25]

(c) DFT GGA [25]

(d) ReaxFF [11]

Figure 4.4: Energy vs. Volume. **Figures do not have the same zero potential energy**

Chapter 5

Potential Energy Surfaces

Potential Energy Surfaces(PES) are useful in determining important information about gas phase interactions with surface, such as energy and location of oxygen adsorption. A PES is formed by varying one or more degree of freedom of a system and recording the potential energy at each location. We will examine two different reactions that are of importance to oxygen catalysis on a silica surface: O-Si bond formation/breaking(adsorption), and O-OSi bond formation/breaking(recombination).

Oxygen Adsorption on β-Cristobalite

Although this work will focus on quartz surfaces, we report potential energy surfaces for oxygen adsorption on β-Cristobalite surface because of the availability of prior computational results. In the ReaxFF training set, Si-O dissociation curves were parametrized from the dissociation of $H_2Si{=}O$, as shown in Fig. 5.1. A comparison of potential energy surfaces in Fig. 5.1 shows that ReaxFF predicts a stronger adsorption minimum, closer to the surface than DFT and hybrid methods. Additionally, we can also see that the long range terms in ReaxFF(Van der Waals and Coulomb) act to attract the atom towards the surface at longer distances. All potential energy scans, referenced or otherwise, were performed by moving an oxygen atom normally above a silicon atom on a frozen (001) Si terminated β-Cristobalite surface. For the PES made using ReaxFF, we used a surface of 10 atomic layers thick with experimental lattice parameters. Thicker surfaces did not change the potential energy. The energy of adsorption could effect the

catalycity of the surface. For example, oxygen atoms that are strongly bound to silicon atoms might be more difficult to remove via recombination. This is just one situation where the force field could be retrained to produce more accurate results. Such PES calculations are therefore important for FF validation.

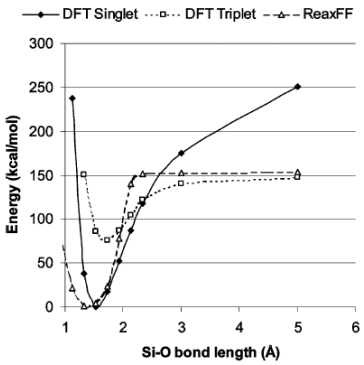

(a) Comparison of ReaxFF and DFT for $H_2Si{=}O$ bond dissociation.

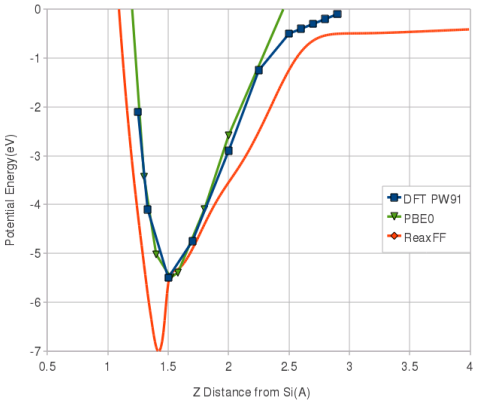

(b) Oxygen Adsorption on (001) β-Cristobalite. Lines: ReaxFF. Squares: DFT-PW91[21]. PBE0 in a similar manner to [19].

Figure 5.1: O-Si bond formation

Oxygen Adsorption on β-Quartz

We also performed a number of one-dimensional potential energy scans of an oxygen atom over a frozen β-quartz(001) surface at a number of likely sites, shown in Fig. 5.2. The PES for adsorption over the T1 site is almost identical to the result for β-Cristobalite. A 3-dimensional potential energy scan of an oxygen atom over the same frozen surface shows that all of the observed minima are just aspects of one large minimum extending over the silicon atom as shown in Fig. 5.3. Furthermore, if an energy minimization is performed at each point on the 3-dimensional PES, allowing all atoms in system to relax except for the adsorbing oxygen, we find a adsorption minimum of 10eV at the bridge sites B1 and B2. This shows why it might be a bad assumption to construct an oxygen-quartz interaction potential based on the interaction of an oxygen

with a frozen surface, as is done in some studies[17].

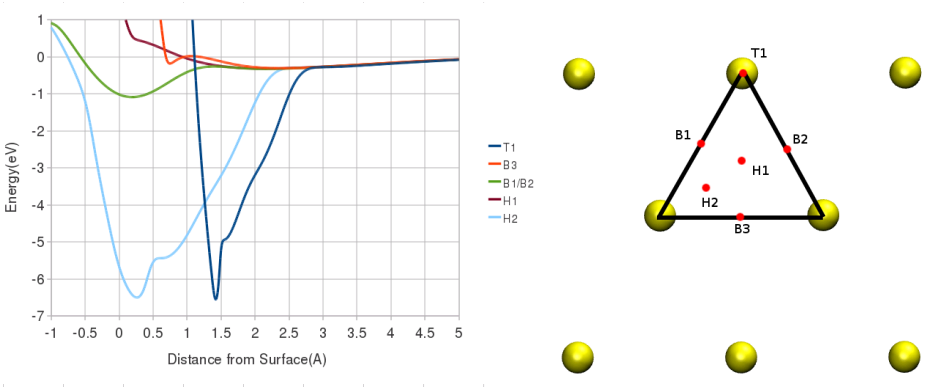

(a) 1-D PES (b) Possible adsorption sites

Figure 5.2: 1-D PES for normal O adsorption on β-quartz

Oxygen Recombination on β-Quartz

In the training of ReaxFF$_{SiO}$, bond dissociation energies for O-O interactions were parametrized from DFT calculations of the dissociation of molecular oxygen and the dissociation of (HO-OH). To determine whether ReaxFF predicts any activation energy for ER recombination on a quartz surface, we computed the PES of an O atom recombining with an adsorbed O atom on a bridge site(B1 or B2 in Fig. 5.2) and on a top site(T1). The surface and the adsorbed oxygen atom were allowed to relax at each step as the oxygen was moved towards the surface. In both cases recombination was energetically favorable(ΔE = -4.5 eV), and there was a small activation energy of .05 eV, as shown in Fig. 5.4. Unfortunately, at this time these is no computational data available for the activation energies of oxygen recombination or adsorption on quartz surfaces.

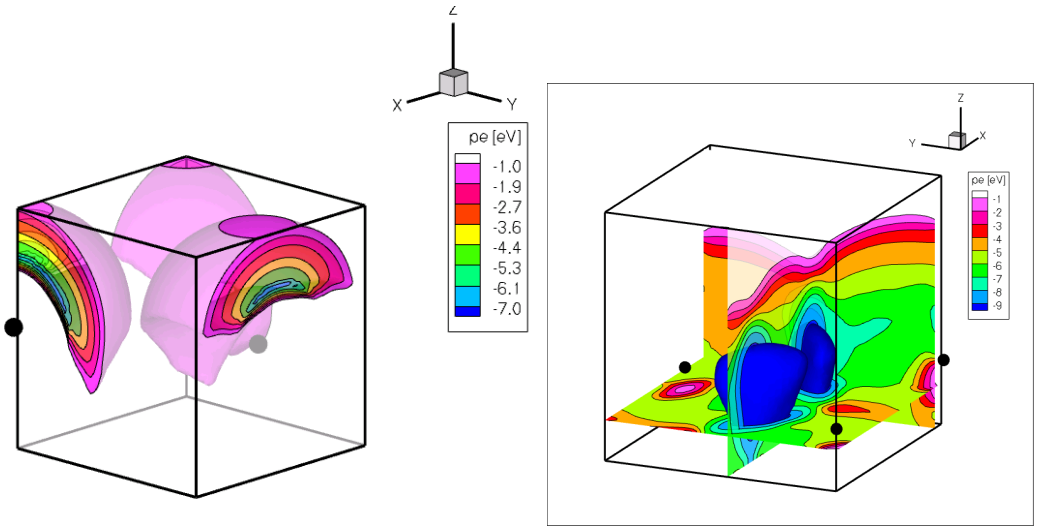

(a) Surface is frozen

(b) Surface is allowed to relax

Figure 5.3: A 3-D PES of a (001) β-Quartz surface. Black spheres represent the original locations of Silicon atoms

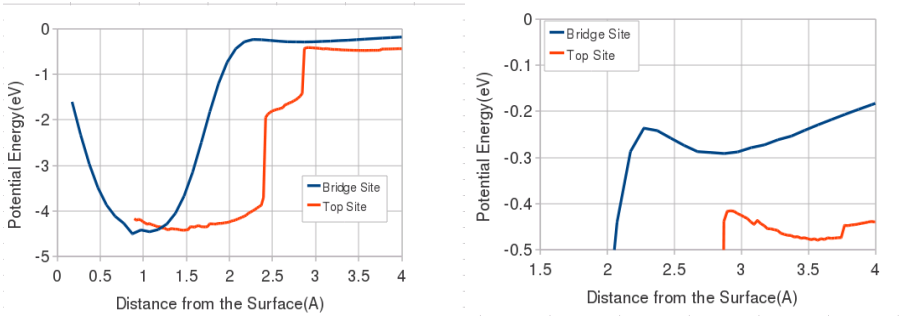

(a) PES of ER O-O recombination

(b) A small barrier of .05 eV is found in both cases

Figure 5.4: ER O-O recombination on a (001) β-Quartz surface

Chapter 6

Molecular Dynamics Simulations

Flux Boundary Condition

In the first work to study surface catalysis on SiO_2 using ReaxFF[2], it was observed that the majority of atomic species in the gas phase adsorbed on an initially vacant surface. When the surface is at equilibrium with the gas phase, one would expect no net mass transfer to the surface. To provide enough atoms in the gas phase to fully populate the surface with NVT molecular dynamics, we would need a very tall column of gas above the surface, or to constantly refresh the gas phase until no net adsorption was seen. We choose the latter, in the form of a flux boundary condition. This approach assumes that the surface is interacting with a uniform, non-changing volume of ideal gas, and allows us to remove gas phase calculations from the simulation. Under this assumption, the number of atoms colliding with the surface(per unit area*time) is given by the flux of an ideal gas through a plane:

$$F = n\overline{C}/4 \tag{6.1}$$

Where n is the number density of molecules and $\overline{C}$ is their average speed. A Poisson distribution based on the expected flux over a given simulation time is used to select the total number molecules added. Molecular additions are distributed randomly over the course of the simulation. Molecules are placed randomly on a plane at 10 Å above the surface, which is beyond the interatomic force cutoff used in our calculations. Any species more than 15 Å from the surface is deleted from the simulation. The translational velocity of impinging molecules is sampled from the Maxwell-Boltzman distribution as

described by Garcia et al.[36]. In cases where diatomic molecules are added to the simulation, their rotational energy is sampled from the rotational energy distribution for a diatomic molecule. Because of the classical nature of the force field, we have neglected vibrational energy, however, this could in principle be added by sampling from the vibrational energy distribution of a harmonic oscillator. The harmonic coefficient predicted by ReaxFF for O_2 was found to be 1268 N/m, which compares reasonably well to the experimentally measured value of 1142 N/m[37].

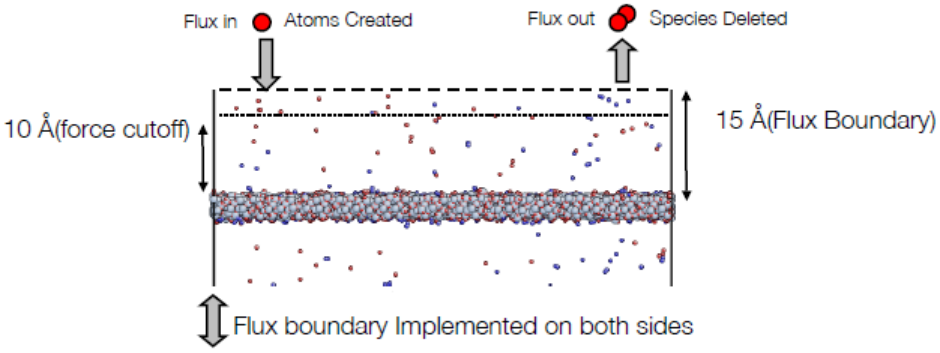

Figure 6.1: Diagram of the Flux boundary condition

Surface Preparation

An idealized surface can be created by copying the unit cell of a crystal in 3D space and cutting along the desired plane of the surface. However, while the bulk crystal structure quartz is known, the atomic geometries and reconstructions on the surface are more difficult to predict because of the covalent character of silica. There are Low Energy Electron Diffraction(LEED)[38, 39] and DFT[40, 41] results that indicate the presence of certain reconstructions on an α-quartz surface under vacuum. However, the catalytic properties of silica samples under experimental conditions can be strongly dependent on the specific plasma conditions, and it has been suggested that plasma conditions can affect the number of active surface sites[42]. Because there is a lack of *in situ* measurements of the surface under experimental conditions, we will use a simple

idealized surface: a β-quartz crystal cut along to (001) plane. For MD simulations, we choose a silicon terminated surface with an area of 2100 $\mathring{A}^2$(which corresponds to 100 exposed Si atoms), as shown in Fig. 6.2. Similarly to Cozmuta[2], during simulations both sides of the surface were exposed gas phase atoms, effectively doubling the area of the surface.

All simulations were run with the LAMMPS[34] molecular dynamics program, with periodicity enforced in the directions perpendicular to the surface. A time step of .5 fs was used, and the verlet algorithm was used for time integration. To prevent the surface from moving or deforming over the course of the simulation, one central layer of the surface was kept fixed. The surrounding two layers were thermalized with the Langevin thermostat, which prevented the surface from heating up from collisions, adsorptions and recombinations. The remaining layers of the surface were allowed to move freely. This approach essentially simulates the heat conduction away from the surface, ensuring a constant surface temperature. As in the work by Cozmuta[2], surfaces were allowed to release stress by dynamically adjusting the planar dimensions using the Nose/Hoover temperature thermostat and pressure barostat for 25ps. The boundaries were then fixed and the simulation was run for 25 ps under Langevin thermostatting before exposing the surface to gas phase atoms.

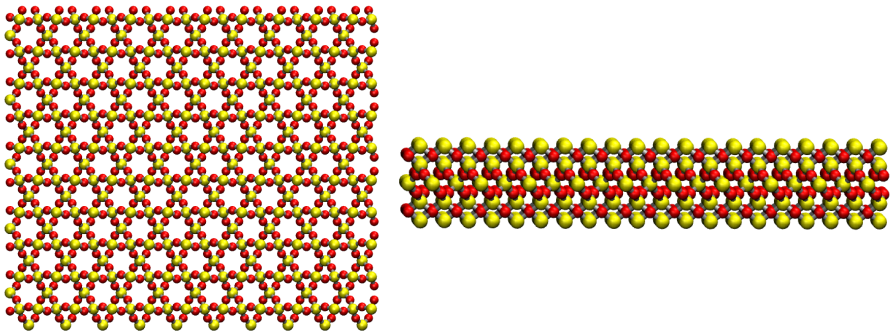

(a) Top View (b) Side View

Figure 6.2: 2100$\mathring{A}$ β-Quartz surface used for MD simulations

Flux Boundary Validation

As an initial test of this method, we applied the flux boundary condition to a domain terminated by specular wall with non-interacting atoms, and found that the number of atoms in the volume obeyed the Ideal Gas Law. For a system of interacting atoms, one foreseeable problem with this method is that at high gas densities, interacting atoms might recombine in the gas phase in the short time before they reach the surface. Also, gas phase atoms are randomly placed on a plane above the surface, so it is entirely possible that atoms can be placed unrealistically close to one another, which could lead to recombination or, in the worst case, an extremely strong repellent force leading to high velocities. To analyze these effects we ran simulations with the flux boundary condition and a specular wall with reactive atomic oxygen at pressures of 10atm and 100atm. The height of the simulation domain was chosen to be 10 Å to resemble simulations with the quartz surface. We measured recombination coefficients from these simulations as:

$$\gamma = \frac{2 * F_{outO_2}}{F_{inO}} \tag{6.2}$$

As shown in Fig. 6.3, there was recombination in the gas phase at both 100atm and 10atm. This error was factored in when calculating recombination coefficients on silica surfaces. At both pressures, the temperature set by the flux boundary condition gave the correct temperature in the gas phase. As expected, recombination coefficients significantly decreased at lower pressures.

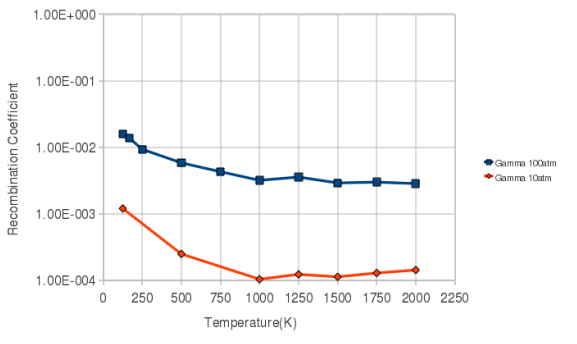

Figure 6.3: Recombination of atomic oxygen at a specular wall

Surface Population

Exposing a vacant surface to a gas is quite unphysical. In reality, some pre-existing surface coverage would accommodate to any change in gas composition almost instantaneously. However, because we have no prior knowledge of the surface coverage, we use the flux boundary condition to expose an initially vacant surface to a gas at a given temperature and pressure. Gas atoms adsorb on the surface, which eventually reaches a steady state composition, as shown in Fig. 6.4. After a steady state coverage has been reached, recombination coefficients can be measured based on the flux towards and away of the surface. Due to relatively long timescale for population(in MD terms), this the most is computationally expensive step. In Fig. 6.4, we can see that population takes much longer at lower pressures.

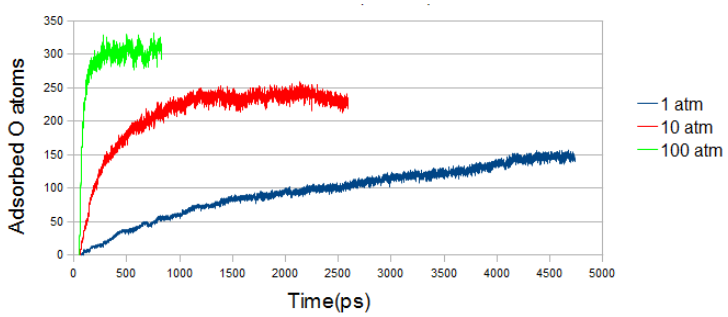

Figure 6.4: Population times at different temperatures

Using LAMMPS in its parallel capacity, a 250 ps simulation for a surface of ∼2000 atoms took about 12hrs on 16 processors. To obtain results in a reasonable amount of time, this sets the lower pressure limit of our method at about 5atm. However, given enough time, lower pressures are technically possible. At lower pressures, it is somewhat difficult to judge whether a surface has finished populating, as shown by the 1 atm line in Fig. 6.4. In all of the proceeding simulations, it appeared that the surfaces had reached a steady state population. However, it is interesting to note the recombination coefficients measured during population did not change significantly when the the number of atoms on the surface was slowly changing with time.

Recombination Coefficients

Using the flux boundary condition, we ran simulations to calculate recombination coefficients for a variety of conditions. Recombination coefficients were measured for a pure atomic oxygen gas at 10 atm and 100atm, as well as for a 50/50 mixture of molecular oxygen and atomic oxygen, as shown in Fig. 6.5. In each case recombination coefficients were collected over the course of 1.5ns. Simulations at (T<250K) for 100atm were not fully populated, however the recombination coefficients did not change significantly as time progressed. Generally, we see that the computed recombination coefficients increase with temperature. They are also much higher than those measured experimentally. Figure 6.6 shows that recombination coefficients at high temperatures follow an exponential trend. The exponential factors are tabulated in Table 6.1. Simulations run with thicker surfaces and larger thermostat layers did not affect any of the above results.

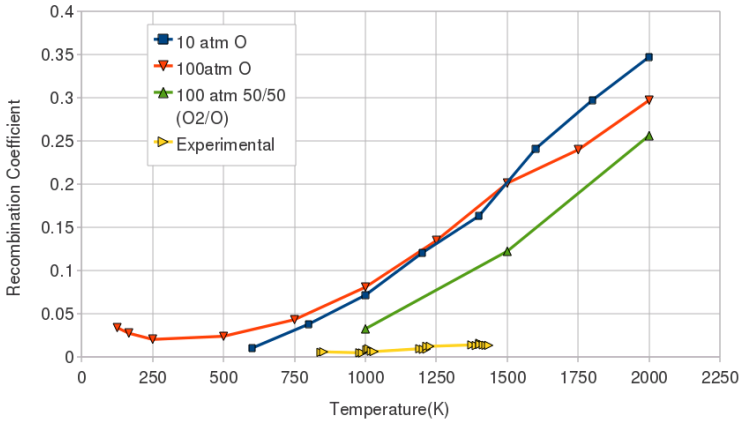

Figure 6.5: γ. Experimental results from [1].

At lower temperatures and at a pressure of 100atm, recombination coefficients reach a minimum and begin to increase. A similar trend is observed in experiment as shown in Fig. 6.7. However, at these conditions the gas density($\sim$ 3 atoms/ $10\mathring{A}^3$ at 250K) is much higher than at experimental conditions, and there are many gas-gas interactions between atoms.

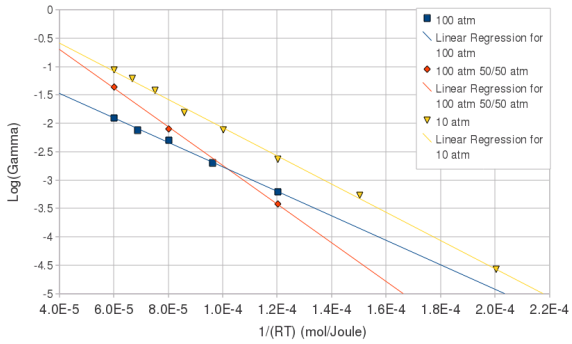

Figure 6.6: Exponential Fit of Recombination Coefficients

Source	Exponential Factor
10 atm pure O Simulation	.26 eV
100 atm 50/50 O2/O Simulation	.35 eV
100 atm pure O Simulation	.22 eV
Kim and Bourdart[6]	.185 ± .006 eV
Balat et al.[1]	.166 ± .02 eV

Table 6.1: Recombination Coefficients vs. Temperature. Experimental results from [1]

In order to determine how recombination coefficients behave at lower pressure, simulations were performed at 2000K from 100atm to 5 atm, as shown in Fig. 6.8. At lower pressures, there is a notable increase in recombination coefficients.

In all the simulations performed, the recombination coefficients are much higher than those measured experimentally. The trend in recombination coefficients with temperature is exponential, which was observed experimentally. The activation energy computed from the exponential trend is higher than the experimentally measured value, and is decreases between 100atm and 10atm cases. In simulations at 100atm, there were a significant amount of gas phase interactions, whereas at 10 atm these are significantly reduced, so it would be more telling to see how the activation energy varied at pressures lower than 10atm. In the case where a 50/50 mixture of O_2/O was used, the recombination coefficients slightly reduced. This is of interest because in some experiments, the

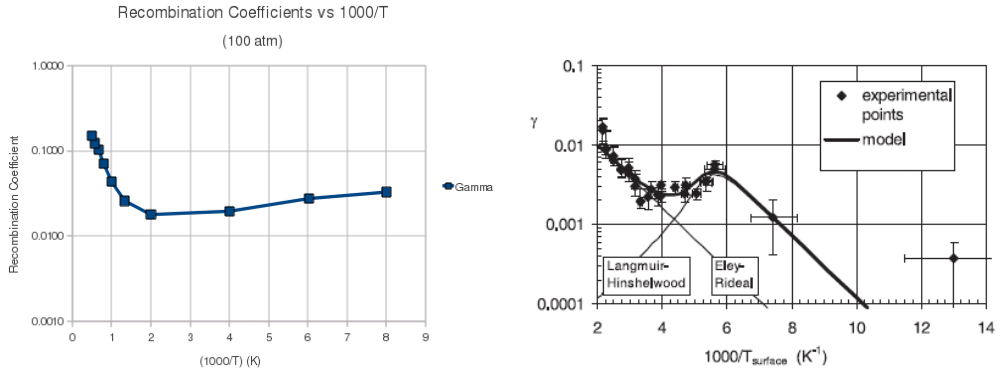

(a) 100 atm

(b) Recombination Coefficients on Pyrex[9].

Figure 6.7: Low Temperature Recombination Coefficients

amount of dissociated O_2 can be as low as 2%[8]. Future work will include measuring how recombination coefficients change with gas composition.

Because we can not fully reproduce experimental conditions it may be somewhat misleading to compare directly to experimental recombination coefficients. There have been many experimental studies to measure recombination coefficients, and the measured values for γ have ranged over several orders of magnitude. For example, the highest(to our knowledge) recombination coefficients for oxygen on silica were measured in an atomic beam experiment performed by Carleton[14]. In this experiment, a sample of reaction cured glass was first cleaned under ultra high vacuum conditions($1x10^{-9}$ Torr) by an atomic beam of 50/50 oxygen/Argon. Under the same conditions, recombination coefficients were measured to range between(.4 at 1000K to .08 at 700K). Reaction cured glass contains 3-7 % B_2O_3, however it has been shown by Jumper et. al that it has a similar catalytic properties to pure silicon dioxide[7]. Moreover, the recombination coefficients measured in this experiment were significantly higher than any other values we found in the literature, but they were measured under different conditions(much lower pressures) with a different experimental technique. Future work will be needed choose which specific experimental setups and conditions are the most realistic to compare against.

To better explain the observed trends in recombination, molecular simulations enable

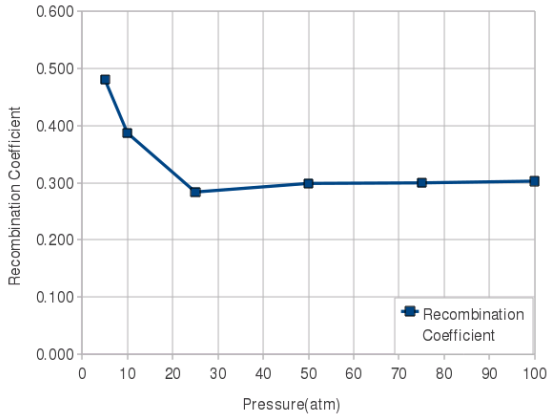

Figure 6.8: Recombination Coefficients vs. Pressure

the examination of surface coverage and the catalytic mechanisms that contribute to recombination.

Surface Coverage

Exposing the quartz surface to the highly reactive atomic gas causes significant reconstructions. The top 2Å of a surface populated with a 10atm 800K atomic oxygen gas is shown in Fig. 6.9. The top view clearly shows a myriad of Si-O membered rings of various sizes. Additionally, there are many O_2 molecules bound to SiO_3 groups on the surface. To characterize which species are on the surface, we define the most common structures seen on the surface in Table 6.2. A bond order cutoff of .5 was used to identify chemically bonded species. Using these definitions we plot the dependence of surface coverage with pressure and temperature in Fig. 6.10.

As temperature decreases, the number of O_2 on the surface increases. As shown in the subsequent section on catalytic mechanisms, nearly all recombined O_2 molecules leaving the surface come from these adsorbed O_2. The drop in recombination coefficients at lower temperatures is due to the fact that molecular O_2 takes longer to desorb at lower temperatures. At lower pressures, the flux of atomic oxygen to the surface is lower, giving O_2 molecules a longer time to desorb between gas phase collisions with the surface. A lower flux to the surface, coupled with a higher flux of O_2 off the surface

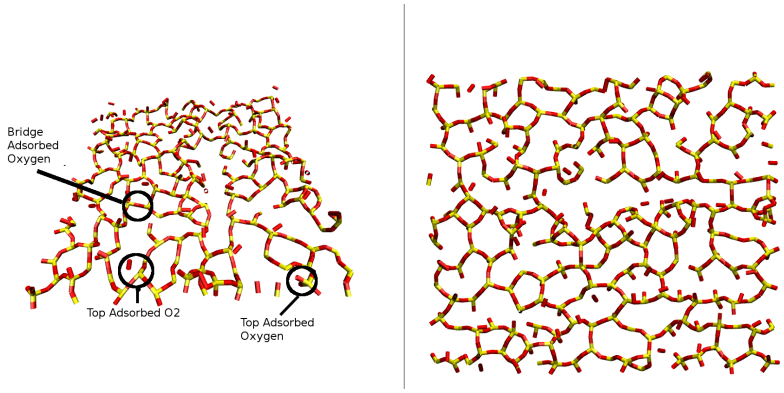

(a) Adsorbed species (b) Top view

Figure 6.9: Disordered SiO_2 at 800K

Name	Description
Top chemisorbed O	O-SiX
Bridge Chemisorbed O	XSi-O-SiX
Top Chemisorbed O_2	O_2Si
Physisorbed O	Atom within 2.5 $\mathring{A}$ of the surface*.
Open Site	Undercoordinated Si atom

*Normalized by numer of atoms expected in the same volume of ideal gas.

Table 6.2: Definitions of various adsorbed species.

between collisions gives higher recombination coefficients at lower pressures. As shown in the subsequent section on catalytic mechanisms, many of the O_2 molecules on the surface are formed by the recombination of gas phase oxygen with top chemisorbed oxygen atoms. Therefore the number of chemisorbed O and O_2 on the surface can be used as an estimate for the number of active sites. Based on experimental results for oxygen recombination on quartz and a mechanism based catalytic model, Guerra estimates that the average distance between active sites on a quartz surface is about 40 Å[43]. On the surface we are using(45x45Å), this would correspond to only a few active sites. For the results at 10atm, there are about 40 active sites in the same area. Thus, the large difference between our recombination coefficients and those measured

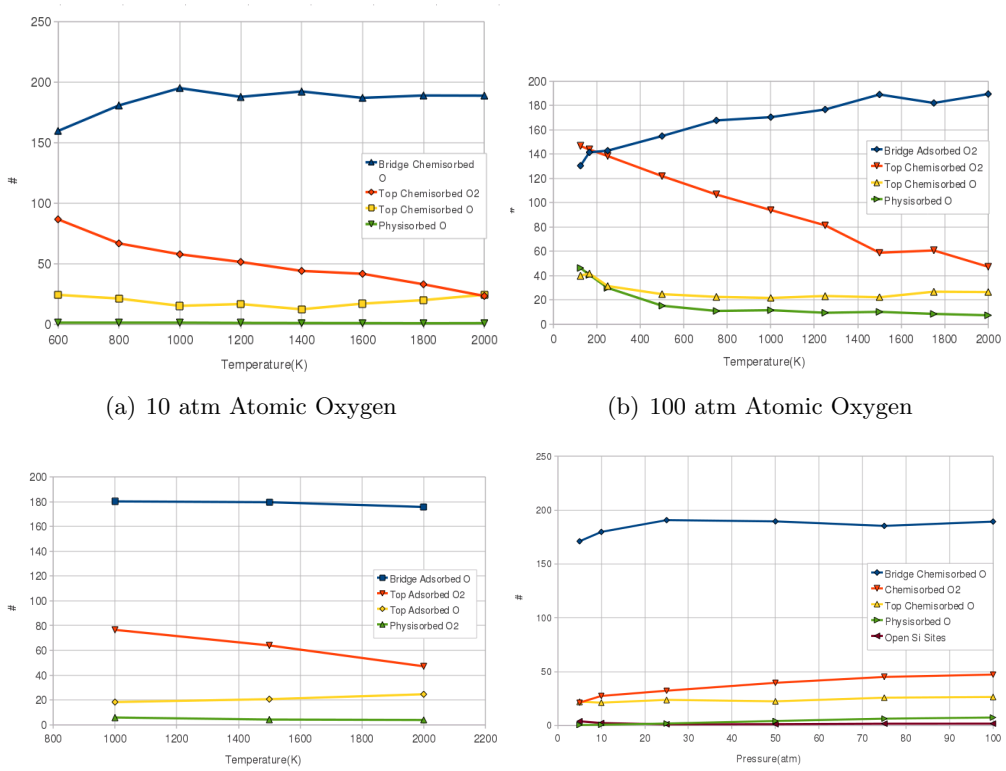

(a) 10 atm Atomic Oxygen

(b) 100 atm Atomic Oxygen

(c) 100 atm 50/50 O_2/O

(d) 2000K Atomic Oxygen

Figure 6.10: Number of species adsorbed on the at various conditions

experimentally could be the number of active sites on the surface.

Catalytic Mechanisms

To analyze how recombination reactions occur on the surface, we take a backwards approach. First, we consider O_2 molecules that flux out of the simulation, and determine their origin. As shown in Table 3.1, there were three primary means for this. An O_2 molecule is defined as adsorbed if it is resident on the same surface site for at least 5ps. Note that for the LH reaction, we do not distinguish where the oxygen atoms are adsorbed(they could be both bonded to the same Si atom, or each bonded to different Si atoms).

As shown in Fig. 6.11, the majority of recombined O_2 molecules fluxing out of the

$O_2(S) \rightarrow O_2 + (S)$	molecular desorption
$O + O(S) \rightarrow O_2 + (S)$	ER recombination
$O(S) + O(S) \rightarrow O_2 + 2(S)$	LH type recombination

Table 6.3: Mechanisms for Surface Catalysis

simulation came from molecular desorption. At 100atm, we see that the ER mechanism contributes more at lower temperatures, and the LH mechanism slightly contributes at higher temperatures. At 10atm, there were fewer O_2 leaving the surface, and there is not enough data to infer any trends.

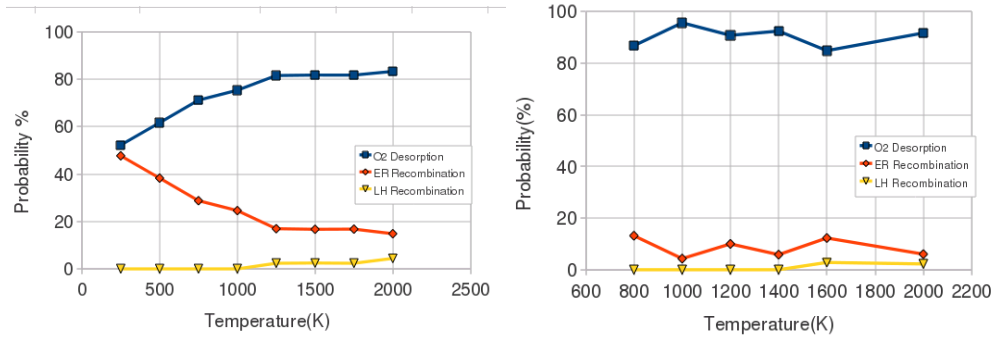

(a) 100 atm Atomic Oxygen

(b) 10 atm Atomic Oxygen

Figure 6.11: Probabilities for Different Mechanisms

An analysis of O_2 formation on the surface shows that both recombination mechanisms in Table 6.3 contribute to O_2 formation, as shown in Fig. 6.12. At 100 atm more O_2 molecules are formed on the surface due to ER recombinations. This makes sense, because at higher pressures the surface is being constantly bombarded with atoms. In both cases, at higher temperatures more O_2 are formed through LH recombination. Because there is a distinct climb in LH recombination with temperature, we expect that there might be an activation energy for this reaction. Future work could involve using potential energy scans to find this activation energy.

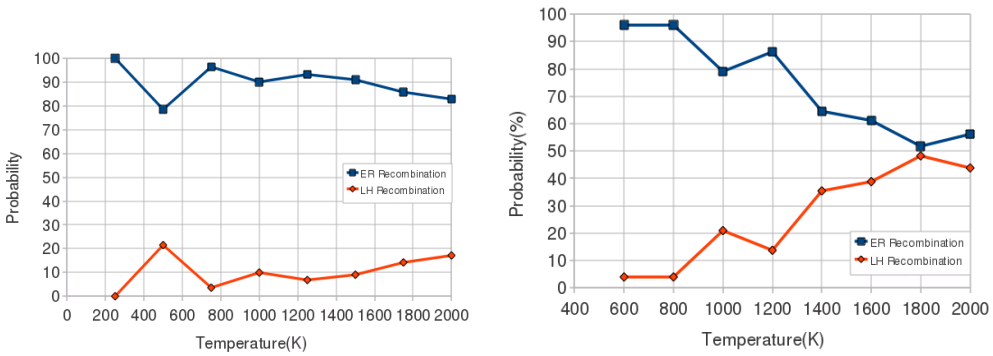

(a) 100 atm Atomic Oxygen

(b) 10 atm Atomic Oxygen

Figure 6.12: Probabilities for Different O_2 Formation Mechanisms

Chapter 7

Conclusion

In this work, we have developed a generic methodology for the validation of the ReaxFF potential and its use to calculate catalytic properties of an SiO_2 surface. Using compression/expansion equation of state calculations and bulk minimizations the predicted crystal structure of SiO_2 can be compared to experimental values. Potential Energy Surfaces can be used to compare ReaxFF to DFT and ab initio results for the energies of various of interactions of interest. Once confidence in the potential is obtained, the flux boundary condition is used to measure recombination coefficients and surface coverages on a silica surface.

Using the above methods we achieved mixed results using the unaltered ReaxFF potential. Bulk calculations showed that ReaxFF accurately predicted the structure of β-quartz but not β-Cristobalite. Potential Energy Surfaces showed that ReaxFF predicted a stronger adsorption minimum for oxygen in β-Cristobalite that DFT results. Thus, there is room for improvement in the force field in these situations. Also, it is evident that we will need more DFT or *ab inito* calculations for some situations of interest(such as oxygen adsorption of β-quartz), to fully validate the potential. The ReaxFF potential is parametrized with QC results, so calculations of these type can be directly incorporated into the training set in order to improve the force field.

The flux boundary condition was adequate for populating a surface at high pressures, however it proved infeasible for the lower pressures($<$1 atm) that are of interest in this problem. In future work, surface population may have to be achieved using a faster means, such as the Grand Canonical Monte Carlo technique. Using the flux

boundary condition, we found recombination coefficients that scaled exponentially with temperature, as was observed experimentally. However, the measured recombination coefficients were much higher than those measured experimentally, and the exponential trend was steeper. Because the simulations were run under conditions that are vastly different from experiments, it is unclear whether our results should agree with experiment. In addition, recombination coefficients in the literature were sensitive to both experimental setup and technique, so some work will be needed to make sure that our conditions and measurement techniques correspond to those in experiment.

References

[1] M. Balat-Pichelin, J.M. Badie, R. Berjoan, and P. Boubert. Recombination coefficient of atomic oxygen on ceramic materials under earth re-entry coinditions by optical emission spectroscopy. *Chemical Physics*, 291:181–194, 2003.

[2] I. Cozmuta. Molecular mechanisms of gas surface interactions in hypersonic flow. Miami, FL, 2007.

[3] M. Barbato, S. Reggiani, C. Bruno, and J. Muylaert. Model for heterogeneous catalysis on metal surfaces with applications to hypersonic flows. *Journal of Thermophysics and Heat Transfer*, 14(3):412–420, 2000.

[4] Deepak Bose, Michael. J. Wright, and Grant E. Palmer. Uncertainty analysis of laminar aeroheating predictions for mars entries. *Journal of Thermophysics and Heat Transfer*, 20(4):652–662, 2006.

[5] J. C. Greaves and J. W. Linnet. The recombination of oxygen atoms at surfaces. *Transactions of the Faraday Society*, 1958.

[6] Y. C. Kim and M. Boudart. Recombination of o, n, and h atoms on silica:kinetics and mechanism. *Langmuir*, 7, 1991.

[7] J. E. Jumper and W. A. Seward. Model for oxygen recombination on reaction cured glass. *Journal of Thermophysics and Heat Transfer*, 8(3):460–465, 1994.

[8] Jochen Marschall. Experimental determination of oxygen and nitrogen recombination coefficients at elevated temperatures using laser-induced flourescence. Baltimore, MD, 1997.

[9] P. Macko, P Vies, and G Cernogora. Study of oxygen atom recombination on a pyrex surface at different wall temperatures by means of time-resolved actinometry in a double pulse discharge technique. *Plasma Sources Science and Technology*, 13:251–262, 2004.

[10] L. Bedra, M. Rutigliano, M. Balat Pichelin, and M. Cacciatore. Atomic oxygen recombination of quatz at high temperature: Experiments and molecular dynamics simulation. *Langmuir*, 22:7208–7216, 2006.

[11] A. C. T. van Duin, A Strachan, S. Stewman, Q. Zhang, and W. A. Goddard III. Reaxff$_{SiO}$ reaxtive force field for silicon and silicon oxide systems. *Journal of Physical Chemistry A*, 107:2802–3811, 2003.

[12] M. Balat-Pichelin, V. L. Kovalev, A. F. Kolesnokov, and A. A. Kropnov. An analysis and predicting the efficiency of atomic oxygen recombination and chemical energy accommodation of heated silica surfaces. *Rarified Gas Dynamics: 24th International Sumposium*, 2005.

[13] A. F. Kolesikov, M. I. Yakushin, I. S. Pershin, and S.A Vasilevsku. Comparatice analysis of the inductive plasmatrons capabilities for thermochemical simulation at the earth an mars atmospheric entry conditions. *11th Int. Conf. Methods for Aerophysical Research*, 2002.

[14] K.L. Carleton and WJ. Marinelli. Spacecraft thermal energy accommodation from atomic recombination. *J. Thermophys. Heat Transfer*, 6:650655, 1992.

[15] L. Bedra and M. J. H. Balat-Pichelin. Comparative modeling study and experimental results of atomic oxygen recombination on silica-based surfaces at high temperature. *Aerospace Science and Technology*, 9:318–328, 2005.

[16] J. Berkowitz. *Catalytic oxygen atom recombination on solid surfaces in: The Structure and Chemistry of Solid Surfaces.* Wiley, New York, 1969.

[17] M. Cacciatore and M. Rutigliano. Eley-rideal and langmuir-hinshelwood recombination coefficients for oxygen on silica surfaces. *Journal of Thermophysics and Heat Transfer*, 13(2), 1999.

[18] M. Rutigliano, A. Piertti, M. Cacciatore, N. Sanna, and V. Barone. N atoms recombination of a silica surface: a global theoretical approach. *Surface Science*, 600:4239–4246, 2006.

[19] M. Rutigliano, C. Zazza, N. Sanna, A. Pieretti, G. Mancini, V. Barone, and M. Cacciatore. Oxygen adsorption on β-cristobalite polymorph: Ab initio modeling and semiclassical time-dependent dynamics. *J. Phys. Chem. A.*, 113, 2009.

[20] C. Arasa, P. Gamallo, and R. Sayos. Adsoprtion of atomic oxygen and nitrogen at β-cristobalite(100): A density fuction theory study. *J. Phys. Chem. B.*, 109:14954–14964, 2005.

[21] C. Arasa, H. F. Busnengo, A. Salin, and R. Sayos. Classical dynamics study of atomic oxygen sticking on the β-cristobalite (100) surface. *Surface Science*, 602:975–985, 2008.

[22] C. Arasa, V. Moron, H. F. Busnengo, and R. Sayos. Eley-rideal reaction dynamics between o atoms on β-cristobalite(100) surface: A new interpolated potential energy surface and classical trajectory study. *Surface Science*, 603:2742–2751, 2009.

[23] O Deutschmann, U. Riedel, and J. Warnatz. Modeling of nitrogen and oxygen recombination on partial catalytic surfaces. *Journal of Heat Transfer*, 117:495–501, 1995.

[24] Paolo Valentini, Thomas E. Schwartzentruber, Graham V. Candler, and Iona Cozmuta. A mechanism-based finite-rate surface catalysis model for simulating reactive flows. San Antonio, TX, 2009.

[25] T. Demuth, Y. Jeavoine, J. Hafner, and J. G. Angyan. Polymorphism in silica studied in the local density and generalized-gradient approximations. *Journal of Physics: Condensed Matter*, 11:3833–3874, 1999.

[26] W. L. Wyckoff. *American Journal of Science*, 9:448, 1925.

[27] W. L. Wyckoff. *Z. Kristallogr*, 62:189, 1925.

[28] T. F. W. Barth. The cristobalite structures: I. high cristobalite. *American Journal of Science*, 23:350, 1932.

[29] W. Nieuwenkamp. *Z. Kristallogr.*, 96:454, 1937.

[30] D.R. Peacor. High-temperature single-crystal study of the cristobalite inversion. *Z. Kristallogr.*, 138:274, 1973.

[31] A. F. Wright and A Leadbetter. The structure of the β-cristobalitephases of sio_2 and $alpo_4$. *Philosophy Magazine*, 31:1391, 1975.

[32] Feng Liu, Stephen H. Garofalini, R. D. King-Smirth, and David Vanderbilt. First-principles studies on structural properties of β-cristobalite. *Physical Review Letters*, 70(18):2750, 1993.

[33] R. W. G. Wyckoff. *Crystal Structures*, volume 1. John Wiley Sons, New York, 1963.

[34] S.J. Plimpton. Fast parallel algorithms for short-range molecular dynamics. *J. Computational Physics*, 117:1–19, 1995. lammps.sandia.gov.

[35] A. F. Wright and M. S. Lehmann. The structure of quartz at 25 and 590c determined by neutron diffraction. *Journal of Solid Stage Chemistry*, 36:371, 1981.

[36] A. Garcia and W. Wagner. Generation of the maxwellian inflow distribution. *Journal of computational physics*, 217:693–708, 2006.

[37] D.A. McQuarrie and J. D. Simon. *Physical Chemistry: A molecular Approach.* University Science Books, 1997.

[38] I. Janossy and M. Menyhard. Leed study of quartz crystals. *Surface Science*, 25:647–649, 1971.

[39] F. Bart, M. Gautier, J. P. Duraud, and M. Henriot. (0010) α-quartz surface, a leed, xanes, and els study. *Surface Science*, 274:317–328, 1992.

[40] T. P. M. Goumans, A., W. A. Bround, C. Richard, and A. Catlowac. Structure and stability of the (001) a-quartz surface. *Phys. Chem. Chem. Phys.*, 9:2146–2152, 2007.

[41] P. E. Lopes, E. Demchuck, and A.D. Mackerell. Reconstruction of the (011) surface on α-quartz: An semiclassical ab initio molecular dynamics study. *International Journal of Quantum Chemistry*, 109:50–64, 2009.

[42] B. F. Gordiets and C. M. Ferreira. Self-consistent model of volume and surface processes in air plasma. *AIAA Journal*, 36(9):1643–1651.

[43] Vasco Guerra. Analytical model of heterogeneous atomic recombination of silicalike surfaces. *IEEE Transactions on Plasma Science*, 35(5), 2007.